

## Article

# Design, Development, and Characterization of Low Distortion Advanced Semitransparent Photovoltaic Glass for Buildings Applications

Mohammad Khairul Basher \*, Mohammad Nur-E Alam  and Kamal Alameh

School of Science, Edith Cowan University, Perth, WA 6027, Australia; nurealam840@gmail.com (M.N.-E.A.); kalameh@bigpond.net.au (K.A.)

\* Correspondence: mkbasher@our.ecu.edu.au

**Abstract:** Aesthetic appearance of building-integrated photovoltaic (BIPV) products, such as semi-transparent PV (STPV) glass, is crucial for their widespread adoption and contribution to the net-zero energy building (NZEB) goal. However, the visual distortion significantly limits the aesthetics of STPV glass. In this study, we investigate the distortion effect of transparent periodic-micropattern-based thin-film PV (PMPV) panels available in the market. To minimize the visual distortion of such PMPV glass panel types, we design and develop an aperiodic micropattern-based PV (APMP) glass that significantly reduces visual distortion. The developed APMP glass demonstrates a haze ratio of 3.7% compared to the 10.7% of PMPV glass. Furthermore, the developed AMPV glass shows an average visible transmittance (AVT) of 58.3% which is around 1.3 times higher than that of AMPV glass (43.8%). Finally, the measured CIELAB values ( $L^* = 43.2$ ,  $a^* = -1.55$ ,  $b^* = -2.86$ ) indicate that our developed AMPV glass possesses excellent color neutrality, which makes them suitable for commercial applications. Based on the characterization results, this study will have a significant impact on the areas of smart window glasses that can play a vital role in developing a sustainable environment and enhancing the aesthetical appearance of net-zero energy buildings (NZEB).

**Keywords:** semitransparent PV; BIPV; NZEB; renewable energy; sustainable energy; environmental safety



**Citation:** Basher, M.K.; Alam, M.N.-E.; Alameh, K. Design, Development, and Characterization of Low Distortion Advanced Semitransparent Photovoltaic Glass for Buildings Applications. *Energies* **2021**, *14*, 3929. <https://doi.org/10.3390/en14133929>

Academic Editor: Carlo Renno

Received: 5 June 2021  
Accepted: 25 June 2021  
Published: 30 June 2021

**Publisher's Note:** MDPI stays neutral with regard to jurisdictional claims in published maps and institutional affiliations.



**Copyright:** © 2021 by the authors. Licensee MDPI, Basel, Switzerland. This article is an open access article distributed under the terms and conditions of the Creative Commons Attribution (CC BY) license (<https://creativecommons.org/licenses/by/4.0/>).

## 1. Introduction

Over the last couple of decades, worldwide energy consumption has increased significantly, mainly due to increases in world population and the industrial revolution. The world population is expected to be nearly 11 billion by the end of 2050. For this large population and ongoing industrialization, the energy demand will soar up to maintain a normal and sustainable lifestyle. It is predicted that the global energy demand will exceed 0.74 billion Tera joule (TJ) by 2040, and this requires the burning of 22.7 billion tons of fossil fuel, mainly anthracite coal [1,2]. Modern buildings and infrastructures, both residential and industrial, are nowadays consuming more energy than what was consumed a decade ago. Further industrialization offers better social and financial benefits to the world population, however, it results in the migration of more and more people from rural to urban areas where a greater amount of global energy is already consumed for living by the buildings and infrastructures [3–5]. In addition to this, around two-thirds of the world's population is predicted to live in metropolitan areas by 2050, where there will be a huge challenge for the governments around the world to meet the large energy demand of densely populated cities [4]. On the other hand, urban planners, environmentalists, and architects are more concerned about the issues of environmental hazards and global warming caused by non-renewable fossil fuel-based energy sources [2]. These non-renewable energy sources (Gas, Coal and Oil) have also been creating devastating challenges, namely the emission of greenhouse gases, pollutants (trace metals, particles,  $\text{NO}_x$ ,  $\text{SO}_2$ ) into the atmosphere,

pollution of water from coal, and uncontrollable ash wastes [5]. These major challenges can be effectively overcome by employing sustainable renewable energy technologies [6]. Solar photovoltaics (PV) is one of the most prominent renewable energy technologies, compared to other available technologies [7].

Recently, the utilization of solar panels in built environments has gained more popularity due to their capability of transforming a house into a power generator [8]. This is performed by integrating PV modules in the building either during or after the construction period. A building-integrated photovoltaics (BIPV) system provides not only electrical and thermal energy but also technical and economical benefits to buildings [9,10]. BIPV systems have recently gained more popularity after the net-zero energy buildings (NZEB) concept was announced by the Directive of the European Parliament (2010/31/EU) [11]. For the NZEB concept, buildings must require extremely low energy that can be obtained from on-site renewable energy sources. The greatest potential of NZEB is the development of smart cities, where energy demand and supply come from renewable energy sources and storage systems implemented in the same city [3]. Therefore, the NZEB goal to realize “a completely zero-carbon built environment” can be achieved using BIPV systems [3,12–14].

Although BIPV systems can generate power cost-effectively when considering both the purpose of electricity generators and building materials [9,15], some modern societies still have a negative opinion regarding the implementation of BIPV technology, mainly because of the limitation of the visual and aesthetical appearance [16–26] that displays black or dark blue colors, depending on the photovoltaic technology used [19,27]. BIPV products featuring visible transparency with acceptable aesthetical color (the apparent visual color captured by normal human eyes) are fascinating for the enhancement of public satisfaction and installation proportion [28–32]. Therefore, it is vital to investigate the problems associated with the development of aesthetically appealing BIPV products and to find innovative solutions for mass production that enables reaching the goal of NZEB, thus saving our environment by reducing the demands of fossil fuel. The two important reasons that limit the adoption of semitransparent BIPV glass products in architectural structures are (i) visual distortion and (ii) conversion efficiency. The most efficient semitransparent BIPV glass is so far made by Advanced Solar Power (ASP)-China [33], which is based on thin-film cadmium telluride (CdTe) PV materials. It has been achieved by partially removing the PV materials using laser micromachining technology to achieve transparency and sunlight-to-electricity conversion simultaneously. The semitransparent PV glass made by ASP is the best choice for BIPV application, however, this type of PV glass exhibits visual distortion which makes the glass blurry due to having narrow PV strips that act as a diffraction grating. To solve this issue, we propose using nonuniform spacing between the PV strips, i.e., aperiodic structure, where the visual distortion can be reduced up to a certain level that is commercially acceptable. No studies have so far been found where aperiodic-micropatterns-based semitransparent thin-film PV modules have been developed using laser micromachining. To the best of our knowledge, this is the first study aimed at designing, developing, and characterizing aperiodic-micropatterns-based semitransparent low distortive thin-film PV glass using laser micromachining.

## 2. Materials and Methods

The development of low distortion advanced semitransparent PV glass will begin with the design of micropattern-like periodic structures as shown in Figure 1a using Coreldraw, a professional vector-based designing software creating high-definition images [34]. The micropattern shown in Figure 1 looks like a complete reddish color in 100% zooming, however, when the zooming percentage increases, it is clear that black gaps exist shown in Figure 1b,c, which are unseen to the naked eye.

It is well known that if the gap between two objects is less than around 50 micrometers, human eyes cannot distinguish the gap, and hence, it perceives the image as one object. This concept has been employed to develop semitransparent PV modules by removing micro-scale areas (red portions) from the thin film materials of the solar glass panel,

thus transmitting a significant amount of light through the glass and converting the remaining portion to electricity, thus achieving transparency and electricity-generation simultaneously.

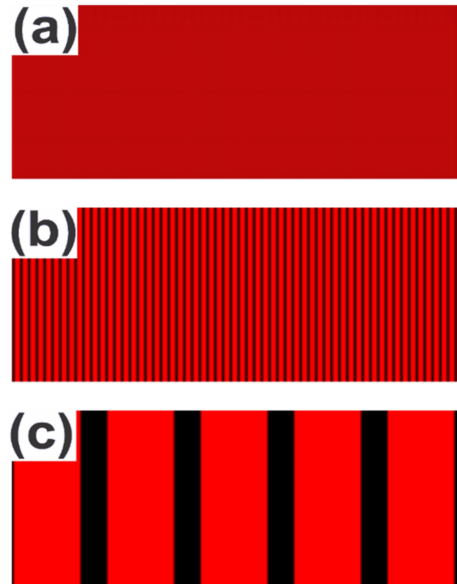


**Figure 1.** Crystalline (periodic) micropattern zooming with 100% (a), 1600% (b) and 18610% (c).

In this article, a laser micromachining system (8020 Trotec Speedy 300 flexx), is used to remove selectively micro-scale areas (red areas) of thin-film PV materials, as illustrated in Figure 1. The fundamental process of laser engraving is a high-energy-density laser pulse irradiating the PV material surface is absorbed and thus increasing the temperature of the PV material, leading to their removal through vaporization [35,36]. However, being transmissive to the laser wavelength, the glass surface on the thin-film PV panel does not get engraved [37]. The laser-machined microstrips (black areas) are typically not seen by the naked eyes but absorb the light incident on them and convert it to electricity. However, periodic micropatterns act as a diffraction grating that typically results in light diffraction (a rainbow effect that causes visual distortion, e.g., haze). This undesired visual distortion can be overcome by using aperiodic micropatterns, as can be seen in Figure 2. Figure 2a illustrates an aperiodic micropatterns on the thin-film PV panel (shown in Figure 2b), where PV area, hence the conversion efficiency of the PV glass is maintained.

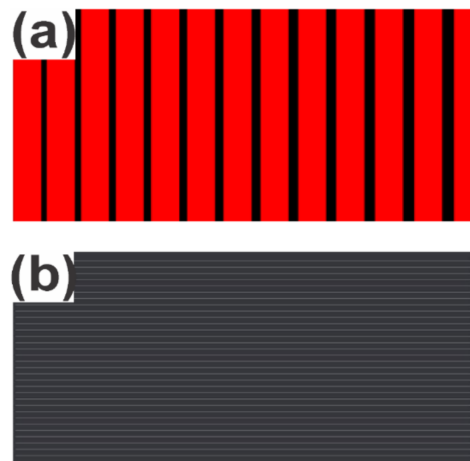


**Figure 2.** Aperiodic Micropattern (a) and thin-film PV panel (b).

The aperiodic patterns was developed by micromaching the PV area to generate PV microstrips of random widths, with the constraint that their overall area is the same as that of the periodic patterns, so that both generate the same electricity, but the aperiodic patterns result in lower grating effect, or distortion. This aperiodic micropatterning approach reduces the visual distortion to a practically adequate level.

A haze meter (Model: SKZ120A, Jinan, Shandong, China) is used to measure the amount of incident light diffracted (optical/visual distortion) when passing through the STPV glasses and these haze values are compared with that of clear glass. Moreover, the diffraction patterns or rainbow effect is visualized more clearly using a camera (Model: STC-P63CJ, SENTECH, Japan) based on the experimental setup shown in Figure 3. Finally, our developed semitransparent PV glasses are characterized using a UV-vis-NIR spectrophotometer (Model: Agilent Cary 5000) for the measurement of transparency, a color-difference meter (Konica Minolta 508D) to determine the color coordinates. These key characteristics' parameters determine the suitability of STPV glass in industrial applications.

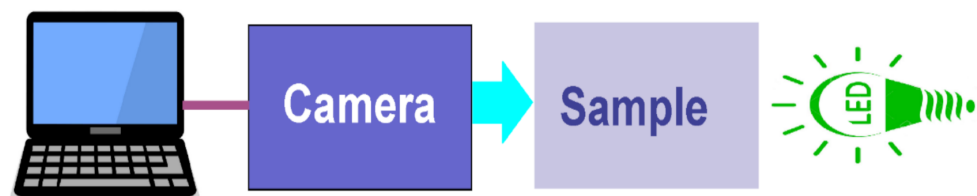


**Figure 3.** Block diagram of the experimental setup to see the diffraction patterns or rainbow effect.

### 3. Results and Discussion

Aesthetical appearance plays a critical role when developing a transparent PV panel. Transparent photovoltaic (TPV) is one of the dominant technologies which significantly enhance the visual appeal of the BIPV system. However, the highly efficient and transparent PV glass available in the market suffers from visual distortion due to the application of periodic micropatterned-based laser engraving [33]. To solve the visual distortion problem, in this study, we have investigated the reason behind having high distortion on PMPV glass. It is found that a high haze value is mainly responsible for the visual distortion of any building-integrated glass products [38]. In TPV application, the haze ratio is important because it reduces the clarity of the PV glass, resulting in blurred vision. To quantitatively evaluate the light diffusion through the TPV, the optical haze (H%) has been calculated using the ratio of the diffuse transmittance ( $T_d$ ) and total transmittance ( $T_t$ ) [38–40]. The haze value determines how much light can travel through a TPV (either dispersed or reflected) that creates blurring features on the backside of the PV glass. Therefore, a lower haze value makes the PV glass less distortive resulting in a clearer view [40]. As a result, a TPV with a low haze value is required, as compared to the transmission haze ratio of glass (less than 1% [38]) for the current and future smart glass and window industries. To reduce the haziness, in this study, we have developed aperiodic micropatterned-based PV (AMPV) glass. The haze ratio for clear glass (CG), PMPV, and AMPV is measured by a Haze meter and presented in Table 1 and Figure 4.

**Table 1.** Haze values of CG, PMPV glass, and AMPV glass.

Sample Name	Haze Ratio
Clear Glass (CG)	0.9%
Periodic Micropatterned based PV (PMPV) glass	10.7%
Aperiodic Micropatterned based PV (AMPV) glass	3.7%

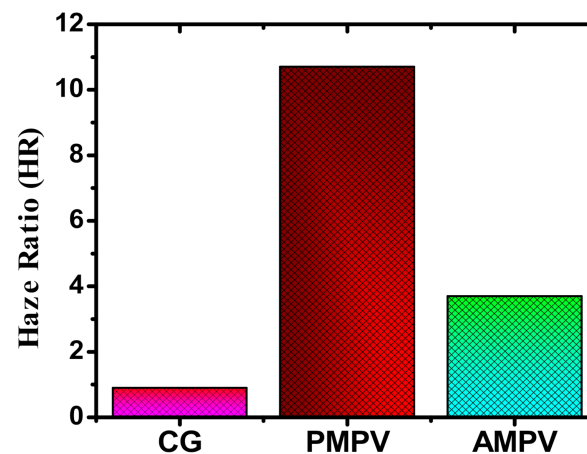


**Figure 4.** Graphical representation of haze values for CG, PMPV glass and AMPV glass.

It can be seen that AMPV glass has a haze ratio of 10.7% which is significantly higher than AMPV glass (3.7%) and CG (0.9%). This is because the periodic micropatterns shown in Figure 5(a1) act as diffraction gratings. It is well known that diffraction gratings are basic optical elements with a specific groove pattern superimposed on them. These tiny, periodic, parallel structures diffract, or diffuse, incident light in such a way that individual wavelengths can be distinguished [41]. Therefore, this diffracted light creates a rainbow effect similar to that of a prism resulting in a visually distorted (e.g., haze) image on the backside of PV glass. This undesired visual distortion is limited by applying aperiodic micropattern as illustrated in Figure 5(b1). The PMPV, and AMPV glasses and their corresponding diffraction patterns and visual images are shown in Figure 5. From Figure 5(a2,b2) which are captured by following the experimental setup shown in Figure 3, it is seen that how the light is diffracted and producing rainbow colors. PMPV glass produces more diffraction effects because periodic micropatterns within it behave as gratings that spread the incoming white light into different angles.

On the other hand, the higher diffraction pattern in Figure 5(a2) is drastically reduced as illustrated in Figure 5(b2) by the application of an aperiodic micropattern. Moreover, the photographs of natural scenery taken through PMPV and AMPV glasses are shown in Figure 5(a3,b3). It is noticeable that PMPV glass produces a blurry image that makes fatigue to the observer or human eyes. On the other hand, AMPV glass creates a visually clear image to the human eyes due to insignificant visual distortion compared to PMPV glass. Therefore, it is observed that AMPV glass reduced the visual distortion to a level (i.e., haziness is 3.7%) that is close to clear glass (i.e., haziness is 0.9%) and reported haze values of ref. [40]. Additionally, the transmission haze ratio of our developed AMPV glass has compatibility with the values reported in refs [38,39].

The visual color appearances of semi-transparent solar cells as seen by human eyes are an important factor in assessing their applicability. The human perception of clarity and color differ from the experimental values obtained from the instruments due to the spectrally based reaction of the human eyes [42]. However, optical transmittance in the visual spectrum determines the visual clarity of glass. Therefore, optical transmittance or average visual transmittance (AVT) plays a significant role to determine the suitability of window glass in buildings and vehicles. The accepted approach for the window industry to reporting AVT is to weigh the integration of the transmission spectrum against the human eye's photopic response [43,44], as follows:

$$AVT = \frac{\int T(\lambda)P(\lambda)S(\lambda)d(\lambda)}{\int P(\lambda)S(\lambda)d(\lambda)} \quad (1)$$

where  $T(\lambda)$  is the transmittance,  $P(\lambda)$  is the photopic response,  $\lambda$  is the wavelength and  $S(\lambda)$  is the solar photon flux (AM1.5G) for window applications or 1 for other applications.

However, when transparent photovoltaic (TPV) is applied in the buildings as window application, AVT is calculated according to the international organization of standardization (ISO) method (ISO 9050:2003), considering the response of the human eye to light in the visible light range (380–780 nm) as follows [39,45,46]:

$$AVT = \frac{\sum_{380}^{780} \tau(\lambda) D_{\lambda} V(\lambda) \Delta\lambda}{\sum_{380}^{780} D_{\lambda} V(\lambda) \Delta\lambda} \quad (2)$$

where  $\tau(\lambda)$  represents the transmittance of PV,  $D_{\lambda}$  represents the spectral distribution of light incident on the PV,  $V_{\lambda}$  represents the sensitivity factor of the eye, and  $\Delta\lambda$  represents the interval of the wavelength.

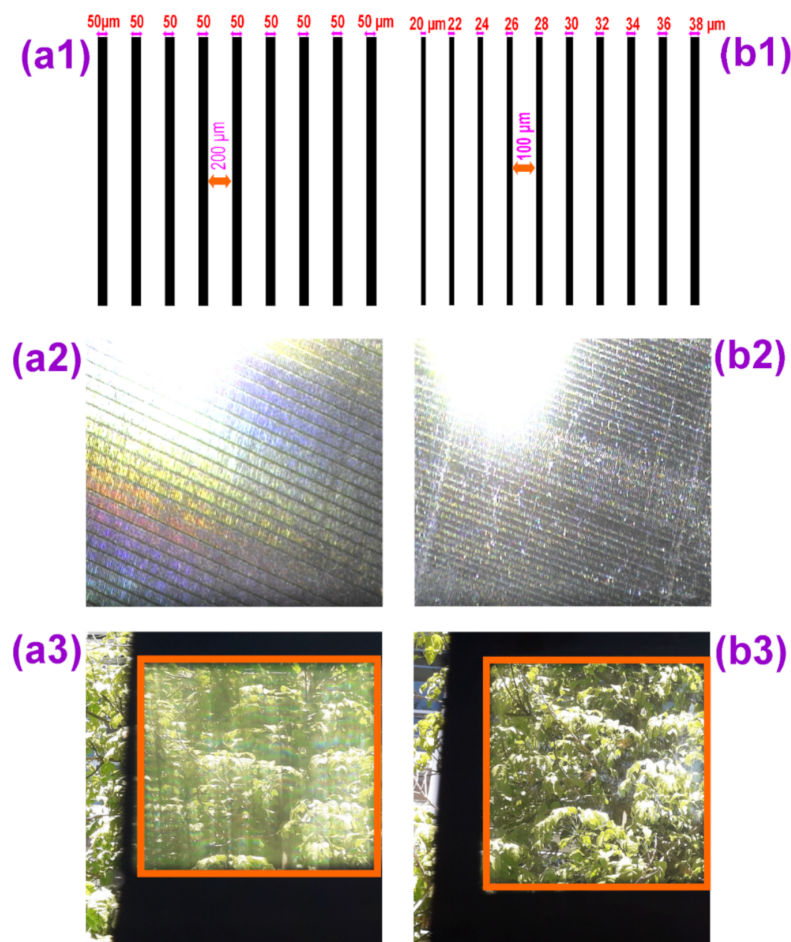


**Figure 5.** (a1) PMPV glass and (b1) AMPV glass, (a2) diffraction pattern of PMPV glass and (b2) diffraction pattern of AMPV glass, and (a3) blurry image through PMPV glass and (b3) clear image through AMPV glass.

The transmittance spectra of clear glass (CG), periodic micropatterned-based PV (PMPV), and aperiodic micropatterned-based PV (AMPV) are shown in Figure 6. The measurement was performed for the visible spectral wavelength range (380–780 nm). The AVT of these three samples is calculated based on the formula reported in ref. [47]. It can be seen from Figure 6 that AMPV glass has more transparency (AVT = 58.7%) than the PMPV glass (AVT = 43.8%). It is reported in ref. [43,48] that any AVT value 60% and above looks clear, which is very close and compatible with the results of our developed AMPV glass. From the transparency point of view, AMPV glass is suitable for commercial uses because the AVT in residential windows can range from 15% for highly tinted glass up to 90% for common clear glass [48].

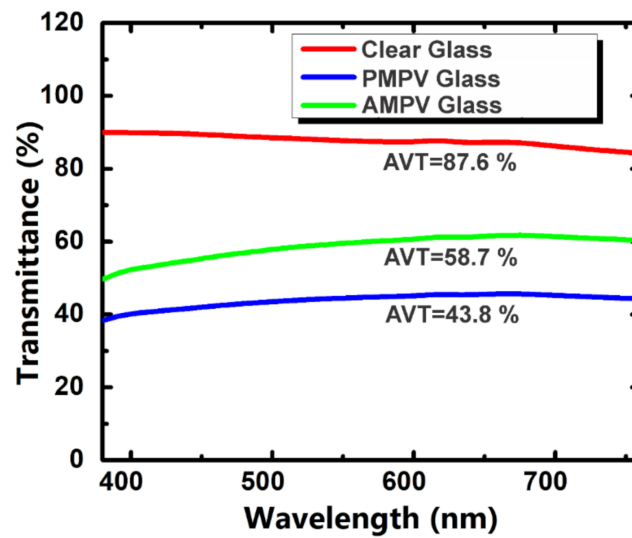


Figure 6. Transmittance spectra of clear glass (CG), PMPV glass, and AMPV glass.

In addition to the haze ratio and transmittance, color perception is also an important factor that needs to point out for the window industry [43]. To accurately evaluate the color perception that is very similar to human vision color sensation, International Commission on Illumination (CIE) recommended several chromaticity diagrams namely CIE 1931 xy, CIE 1971 uv, and CIELAB, etc. for the window industry. However, CIELAB (CIE  $L^*a^*b^*$ ) color coordinate system is the most comprehensive color space that displays not only chromaticity but also brightness values [49,50]. For this reason, we measured the color coordinates (shown in Figure 7) by color spectrophotometer in the CIELAB system. In Figure 7, the brightness ( $L^*$ ) represents the human sense of contrast, with a value of 0 representing complete black and 100 representing complete white, while green to red is represented by the value  $a^*$ , and blue to yellow is represented by the value  $b^*$ . It is reported in the Refs. [39,47,51] that the color is more neutral when the values of  $a^*$  and  $b^*$  are closer to (0,0). The color values for PMPV glass are  $L^* = 48.0$ ,  $a^* = -2.21$ ,  $b^* = -2.46$  whereas APMPV glass has values of  $L^* = 43.2$ ,  $a^* = -1.55$ ,  $b^* = -2.86$ .

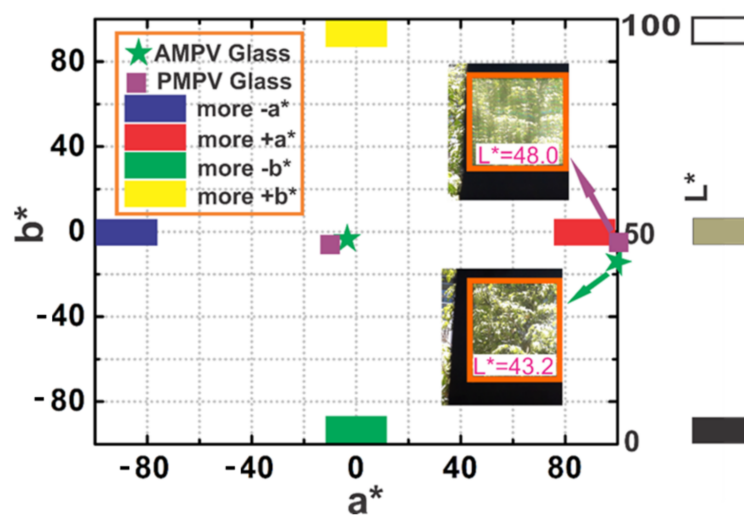


Figure 7. CIELAB values of PMPV and AMPV glasses.

It can be noticed that the brightness ( $L^*$ ) values for both PMPV and APMPV glasses are less than 50 since black microstrips are present in the PV glasses, although these are not visible to human eyes. However, the color coordinates ( $a^*$ ,  $b^*$ ) for both PV glasses are negative values and very close to (0,0). The color coordinates of our STPV glasses

also have compatibility with the other chromaticity diagram of the semitransparent solar cells reported in refs. [42,52]. It is seen that applying aperiodic micropatterns have no noticeable effect on the color coordinates except for little changes in the lightness value. These color values ( $a^*$  and  $b^*$ ) indicated that our developed PV glasses possess excellent color neutrality which is suitable for industrial applications. This is because, in modern window applications, (yellow/red), high positive values of  $a^*$  and  $b^*$  are less frequent, while values near the origin (neutral/grey) and negative values of  $b^*$  (blue) are more common if followed by high AVT [43].

Characterization is crucial after product development. However, in the case of semi-transparent or transparent BIPV products, no standard characterization methods have so far been developed. Nevertheless, researchers agreed on the following three main perspectives that should be considered for the commercialization of BIPV products, namely: (1) high-power conversion efficiency at similar visible transmittance; (2) aesthetic factors, i.e., acceptable detraction, especially for construction and automobile applications; and (3) feasibility for real-world applications, including modularization and stability [39]. Since in this study, we focus solely on the aesthetic aspect of TPV modules, characterization was focused on the aesthetical parameters, such as haze ratio, optical transparency, and color neutrality. From the characterization parameters, it is seen that our developed APMP-based PV glass samples possess very low haze, high AVT, and excellent color neutrality, and these make them suitable for BIPV applications.

#### 4. Conclusions

In conclusion, we have demonstrated the design and development of a visually low distortive semitransparent photovoltaic (PV) glass by means of simple and cost-effective processes suitable for building integrated window applications. To reduce the visual distortion, we have applied aperiodic micropatterns that disrupt the grating properties and produced a very low distortion effect. To the best of our knowledge, this study can mitigate the visual distortion of periodic micropattern-based thin-film solar panels thus can benefit modern glass and window manufacturers. Furthermore, our developed AMPV glass possessed excellent optical transparency and color neutrality which is significantly important for the aesthetical appealing of BIPV products for various applications such as high-rise building construction, cars, greenhouses, and agrophotovoltaic. Additionally, it will play an important role in the widespread application of net-zero energy building (NZEB) that ensures environmental sustainability.

**Author Contributions:** Conceptualization, M.K.B. and K.A.; methodology, M.K.B. and K.A.; software, M.K.B.; validation, M.K.B. and K.A.; formal analysis, M.K.B. and M.N.-E.A.; investigation, M.K.B.; resources, M.K.B. and K.A.; data curation, M.K.B.; writing—original draft, M.K.B.; writing—review and editing, M.K.B., M.N.-E.A. and K.A.; visualization, M.K.B. and M.N.-E.A.; supervision, K.A.; project administration, M.K.B. and K.A. All authors have read and agreed to the published version of the manuscript.

**Funding:** This research received no external funding.

**Institutional Review Board Statement:** Not applicable.

**Informed Consent Statement:** Not applicable.

**Data Availability Statement:** The datasets generated and/or analysed during this study are available from the corresponding author on reasonable request.

**Acknowledgments:** The research was supported by Edith Cowan University (ECU), Australia. The authors wish to thank Mikhail Vasiliev, Paul Roach, our colleagues at Edith Cowan University for their support on preparing the manuscript.

**Conflicts of Interest:** The authors declare no conflict of interest.

## Abbreviations

Advanced Solar Power	ASP
Aperiodic micropattern-based photovoltaic	AMPV
Average visible transmittance	AVT
Building integrated photovoltaic	BIPV
Cadmium telluride	CdTe
Clear glass	CG
International Commission on Illumination	CIE
International organization of standardization	ISO
Micrometers	Mm
Net-zero energy building	NZEB
Nitrogen oxides	NOx
Periodic-micropattern-based photovoltaic	PMPV
Photovoltaic	PV
Semitransparent photovoltaic	STPV
Sulfur dioxide	SO <sub>2</sub>
Tera joule	TJ
Transparent photovoltaic	TPV

## References

1. Tripathy, M.; Sadhu, P.K.; Panda, S. A critical review on building integrated photovoltaic products and their applications. *Renew. Sustain. Energy Rev.* **2016**, *61*, 451–465. [\[CrossRef\]](#)
2. Vasiliev, M.; Alameh, K. Recent developments in solar energy-harvesting technologies for building integration and distributed energy generation. *Energies* **2019**, *12*, 1080. [\[CrossRef\]](#)
3. Attia, S. *Net Zero Energy Buildings (NZEB): Concepts, Frameworks and Roadmap for Project Analysis and Implementation*; Elsevier: San Diego, CA, USA, 2018.
4. Owusu, P.A.; Asumadu-Sarkodie, S. A review of renewable energy sources, sustainability issues and climate change mitigation. *Cogent Eng.* **2016**, *3*. [\[CrossRef\]](#)
5. Asumadu-Sarkodie, S.; Owusu, P.A. Feasibility of biomass heating system in Middle East Technical University, Northern Cyprus Campus. *Cogent Eng.* **2016**, *3*. [\[CrossRef\]](#)
6. Edenhofer, O.; Madrugá, R.P.; Sokona, Y.; Seyboth, K.; Matschoss, P.; Kadner, S.; Zwickel, T.; Eickemeier, P.; Hansen, G.; Schlömer, S.; et al. *Renewable Energy Sources and Climate Change Mitigation*; Cambridge University Press: Cambridge, UK, 2011; ISBN 9781139151153.
7. Kumar, N.M.; Sudhakar, K.; Samykano, M. Performance comparison of BAPV and BIPV systems with c-Si, CIS and CdTe photovoltaic technologies under tropical weather conditions. *Case Stud. Therm. Eng.* **2019**, *13*, 100374. [\[CrossRef\]](#)
8. Snow, M.; Prasad, D. *Designing with Solar Power: A Source Book for Building Integrated Photovoltaics (BIPV)*; Routledge: London, UK, 2005; pp. 1–128.
9. Eder, G.; Peharz, G.; Trattig, R.; Bonomo, P.; Saretta, E.; Frontini, F.; Polo López, C.S.; Rose Wilson, H.; Eisenlohr, J.; Martin Chivelet, N.; et al. *Coloured BIPV-Market, Research and Development*; International Energy Agency: Paris, France, 2019; p. 60.
10. Jelle, B.P. Building integrated photovoltaics: A concise description of the current state of the art and possible research pathways. *Energies* **2015**, *9*, 21. [\[CrossRef\]](#)
11. EUR-Lex. Document 02010L0031-20181224. Available online: <https://eur-lex.europa.eu/eli/dir/2010/31/2018-12-24> (accessed on 13 April 2020).
12. Wong, P.; Shimoda, Y.; Nonaka, M.; Inoue, M.; Mizuno, M. Semi-transparent PV: Thermal performance, power generation, daylight modelling and energy saving potential in a residential application. *Renew. Energy* **2008**, *33*, 1024–1036. [\[CrossRef\]](#)
13. Peng, J.; Curcija, D.C.; Lu, L.; Selkowitz, S.E.; Yang, H.; Zhang, W. Numerical investigation of the energy saving potential of a semi-transparent photovoltaic double-skin facade in a cool-summer Mediterranean climate. *Appl. Energy* **2016**, *165*, 345–356. [\[CrossRef\]](#)
14. Bayoumi, M. Impacts of window opening grade on improving the energy efficiency of a façade in hot climates. *Build. Environ.* **2017**, *119*, 31–43. [\[CrossRef\]](#)
15. Ballif, C.; Perret-Aebi, L.-E.; Lufkin, S.; Rey, E. Integrated thinking for photovoltaics in buildings. *Nat. Energy* **2018**, *3*, 438–442. [\[CrossRef\]](#)
16. Cohen, J.J.; Reichl, J.; Schmidthaler, M. Re-focussing research efforts on the public acceptance of energy infrastructure: A critical review. *Energy* **2014**, *76*, 4–9. [\[CrossRef\]](#)
17. Mittag, M.; Kutter, C.; Ebert, M.; Wilson, H.R.; Eitner, U. Power loss through decorative elements in the front glazing of BIPV modules. In Proceedings of the 33rd European PV Solar Energy Conference and Exhibition, Amsterdam, The Netherlands, 25–29 September 2017.

18. Probst, M.M.; Roecker, C. Criteria for architectural integration of active solar systems IEA task 41, subtask A. *Energy Procedia* **2012**, *30*, 1195–1204. [[CrossRef](#)]
19. Tabakovic, M.; Fechner, H.; van Sark, W.; Louwen, A.; Georghiou, G.; Makrides, G.; Loucaidou, E.; Ioannidou, M.; Weiss, I.; Arancon, S.; et al. Status and outlook for building integrated photovoltaics (BIPV) in relation to educational needs in the BIPV Sector. *Energy Procedia* **2017**, *111*, 993–999. [[CrossRef](#)]
20. Goh, K.C.; Goh, H.H.; Yap, A.B.K.; Masrom, A.N.; Mohamed, S. Barriers and drivers of Malaysian BIPV application: Perspective of developers. *Procedia Eng.* **2017**, *180*, 1585–1595. [[CrossRef](#)]
21. Yang, R.J.; Zou, P. Building integrated photovoltaics (BIPV): Costs, benefits, risks, barriers and improvement strategy. *Int. J. Constr. Manag.* **2016**, *16*, 39–53. [[CrossRef](#)]
22. Karakaya, E.; Sriwannawit, P. Barriers to the adoption of photovoltaic systems: The state of the art. *Renew. Sustain. Energy Rev.* **2015**, *49*, 60–66. [[CrossRef](#)]
23. Yang, R.J. Overcoming technical barriers and risks in the application of building integrated photovoltaics (BIPV): Hardware and software strategies. *Autom. Constr.* **2015**, *51*, 92–102. [[CrossRef](#)]
24. Azadian, F.; Radzi, M.A.M. A general approach toward building integrated photovoltaic systems and its implementation barriers: A review. *Renew. Sustain. Energy Rev.* **2013**, *22*, 527–538. [[CrossRef](#)]
25. Taleb, H.; Pitts, A. The potential to exploit use of building-integrated photovoltaics in countries of the Gulf Cooperation Council. *Renew. Energy* **2009**, *34*, 1092–1099. [[CrossRef](#)]
26. Prieto, A.; Knaack, U.; Auer, T.; Klein, T. Solar façades—Main barriers for widespread façade integration of solar technologies. *J. Facade Des. Eng.* **2017**, *5*, 51–62. [[CrossRef](#)]
27. Scognamiglio, A.; Privato, C. Starting points for a new cultural vision of BIPV. In Proceedings of the 23rd European Photovoltaic Solar Energy Conference and Exhibition, Valencia, Spain, 1–5 September 2008; pp. 3222–3233.
28. Lee, K.-T.; Lee, J.Y.; Seo, S.; Guo, L.J. Colored ultrathin hybrid photovoltaics with high quantum efficiency. *Light Sci. Appl.* **2014**, *3*, e215. [[CrossRef](#)]
29. Lien, S.-Y. Artist photovoltaic modules. *Energies* **2016**, *9*, 551. [[CrossRef](#)]
30. Attoye, D.E.; Aoul, K.A.T.; Hassan, A. A review on building integrated photovoltaic façade customization potentials. *Sustainability* **2017**, *9*, 2287. [[CrossRef](#)]
31. Peharz, G.; Berger, K.; Kubicek, B.; Aichinger, M.; Grobbauer, M.; Gratzer, J.; Nemitz, W.; Großschädl, B.; Auer, C.; Prietl, C.; et al. Application of plasmonic coloring for making building integrated PV modules comprising of green solar cells. *Renew. Energy* **2017**, *109*, 542–550. [[CrossRef](#)]
32. Soman, A.; Antony, A. Colored solar cells with spectrally selective photonic crystal reflectors for application in building integrated photovoltaics. *Sol. Energy* **2019**, *181*, 1–8. [[CrossRef](#)]
33. Calyxo. *CDTE Thin Film Solar Module CX1*; Calyxo: Bitterfeld-Wolfen, Germany, 2011.
34. The Ultimate Guide to Vector Software. CorelDRAW. Available online: <https://www.coreldraw.com/en/tips/vector-images/vector-software/> (accessed on 21 June 2021).
35. How Do Lasers Work—Basics. Available online: <https://www.troteclaser.com/en/faqs/how-does-a-laser-work/> (accessed on 10 September 2020).
36. Working Principle of Laser Marking Machine. Available online: <https://www.xtlaser.com/for-new-user-working-principle-of-fiber-laser-marking-machine-max-from-xt-laser/> (accessed on 10 September 2020).
37. Laser Engraving Glass. Available online: <https://www.engraversjournal.com/legacyarticles/2360/> (accessed on 10 September 2020).
38. Hwang, I.; Choi, D.; Lee, S.; Seo, J.H.; Kim, K.-H.; Yoon, I.; Seo, K. Enhancement of light absorption in photovoltaic devices using textured polydimethylsiloxane stickers. *ACS Appl. Mater. Interfaces* **2017**, *9*, 21276–21282. [[CrossRef](#)]
39. Lee, K.; Um, H.-D.; Choi, D.; Park, J.; Kim, N.; Kim, H.; Seo, K. The development of transparent photovoltaics. *Cell Rep. Phys. Sci.* **2020**, *1*, 100143. [[CrossRef](#)]
40. Lee, K.; Kim, N.; Kim, K.; Um, H.-D.; Jin, W.; Choi, D.; Park, J.; Park, K.J.; Lee, S.; Seo, K. Neutral-colored transparent crystalline silicon photovoltaics. *Joule* **2020**, *4*, 235–246. [[CrossRef](#)]
41. Gratings Separate the Different Colors of Light—Laser Focus World. Available online: <https://www.laserfocusworld.com/optics/article/16550914/gratings-separate-the-different-colors-of-light> (accessed on 10 September 2020).
42. Chen, K.-S.; Salinas, J.-F.; Yip, H.-L.; Huo, L.; Hou, J.; Jen, A.K.-Y. Semi-transparent polymer solar cells with 6% PCE, 25% average visible transmittance and a color rendering index close to 100 for power generating window applications. *Energy Environ. Sci.* **2012**, *5*, 9551–9557. [[CrossRef](#)]
43. Traverse, C.J.; Pandey, R.; Barr, M.C.; Lunt, R.R. Emergence of highly transparent photovoltaics for distributed applications. *Nat. Energy* **2017**, *2*, 849–860. [[CrossRef](#)]
44. Lunt, R.R. Theoretical limits for visibly transparent photovoltaics. *Appl. Phys. Lett.* **2012**, *101*, 043902. [[CrossRef](#)]
45. Colonna, D.; Capogna, V.; Lembo, A.; Brown, T.M.; Reale, A.; Di Carlo, A. Efficient cosensitization strategy for dye-sensitized solar cells. *Appl. Phys. Express* **2012**, *5*, 022303. [[CrossRef](#)]
46. Saifullah, M.; Gwak, J.; Yun, J.H. Comprehensive review on material requirements, present status, and future prospects for building-integrated semitransparent photovoltaics (BISTPV). *J. Mater. Chem. A* **2016**, *4*, 8512–8540. [[CrossRef](#)]

47. Yang, C.; Liu, D.; Bates, M.; Barr, M.C.; Lunt, R.R. How to accurately report transparent solar cells. *Joule* **2019**, *3*, 1803–1809. [[CrossRef](#)]
48. Fisette, P. Windows: Understanding Energy Efficient Performance. 2003. Available online: <https://bct.eco.umass.edu/publications/articles/windows-understanding-energy-efficient-performance/> (accessed on 10 September 2020).
49. CIELAB Color Space—Wikipedia. Available online: [https://en.wikipedia.org/wiki/CIELAB\\_color\\_space](https://en.wikipedia.org/wiki/CIELAB_color_space) (accessed on 10 September 2020).
50. Myong, S.Y.; Jeon, S.W. Design of esthetic color for thin-film silicon semi-transparent photovoltaic modules. *Sol. Energy Mater. Sol. Cells* **2015**, *143*, 442–449. [[CrossRef](#)]
51. Tang, Y.; Cai, W.; Xu, B. Profiles of phenolics, carotenoids and antioxidative capacities of thermal processed white, yellow, orange and purple sweet potatoes grown in Guilin, China. *Food Sci. Hum. Wellness* **2015**, *4*, 123–132. [[CrossRef](#)]
52. Colsmann, A.; Puetz, A.; Bauer, A.; Hanisch, J.; Ahlswede, E.; Lemmer, U. Efficient semi-transparent organic solar cells with good transparency color perception and rendering properties. *Adv. Energy Mater.* **2011**, *1*, 599–603. [[CrossRef](#)]